JOURNAL OF AEROSPACE COMPUTING, INFORMATION, AND COMMUNICATION
Vol. 4, November 2007

Data Mining for Multidisciplinary Design Space of Regional-Jet Wing

Kazuhisa Chiba*
Japan Aerospace Exploration Agency, Tokyo 182-8522, Japan

and

Shigeru Obayashi†
Tohoku University, Sendai 980-8577, Japan

DOI: 10.2514/1.19404

Two data mining techniques have been performed for a large-scale and real-world multidisciplinary design optimization (MDO) results to provide knowledge in design space. The MDO among aerodynamics, structures, and aeroelasticity for a regional-jet wing was carried out using high-fidelity evaluation tools on adaptive range multi-objective genetic algorithm. MDO generated 130 solutions included in nine non-dominated solutions. All solutions were investigated regarding tradeoffs among three objective functions and effects of design variables on objective functions using a self-organizing map (SOM) and a functional analysis of variance (ANOVA) to extract key features of the design space. Consequently, as SOM and ANOVA compensated with respective disadvantages, the design knowledge could be obtained more clearly by the combination between them. Although the MDO result showed the inverted gull-wings as non-dominated solutions, one of the key features revealed by data mining was the non-gull wing geometry. When this knowledge was applied to one optimum solution, the resulting design was found to have better performance compared with the original geometry designed in the conventional manner. Data mining can discover better design due to the salvage of information from design space even when optimization itself does not converge.

I. Introduction

RECENTLY, the design optimization using high-fidelity evaluation models becomes one of the essential tools for aircraft design. Optimization problems are concentrated only on finding the optimal solution. Although a design optimization is important for engineering, the most significant point is the extraction of the knowledge in design space. The results obtained by multi-objective optimization are not a sole solution but an optimum set. That is, as multi-objective optimization result is insufficient information for practical design because designers need a conclusive shape. However, the result of multi-objective optimization can be accounted as a hypothetical design data base. Data mining as a post-process for an optimization is essential to efficiently find useful design knowledge such as tradeoffs and effect of design variable.[1] The design information directly helps the designer determine the next geometry. The process to extract information from a database, which denotes optimization result in this study, is called as data mining. This technique is an important facet of solving and visualizing optimization problem.[2]

Received 9 August 2005; revision received 20 July 2007; accepted for publication 28 September 2007.

* Project Researcher, Civil Transport Team, Aviation Program Group. Member AIAA.
† Professor, Institute of Fluid Science. Associate Fellow AIAA.

Self-organizing map (SOM) is a neural network model suggested by Kohonen.[3] It can serve as an analytical tool for high-dimensional data. The cluster analysis of characteristic values, for example objective functions and design variables, will help to identify tradeoff and effect of design variable. SOM identifies qualitative data description. On the other hand, a functional analysis of variance (ANOVA)[4] decompose a total variance of model into variance component due to each design variable to identify the effect of design variable to objective function. Design variables that have important effect on objective function and characteristic functions can be identified quantitatively using ANOVA. In this study, the above two data mining techniques are applied to a large-scale and real-world MDO problem for a regional jet aircraft design,[5] providing knowledge in the multidisciplinary design space. The objective of this study is to gain beneficial knowledge in the design space by applying data mining which is an emerging are of computational intelligence. Moreover, the features of applied data mining techniques are revealed.

II. MDO Problem

A. Objective Functions

In this system, three objective functions were defined: (1) minimization of the block fuel at a required target range derived from aerodynamics and structure mechanics was selected as a primary objective function. In addition, two more objective functions were considered—(2) minimization of the maximum takeoff weight and (3) minimization of the difference in the drag coefficient C_D between two Mach numbers, which are cruise Mach and target Maximum Operating Mach number (MMO), to prevent decrease in MMO.

B. Geometry Definition

First, the planform was given by Mitsubishi Heavy Industries, Ltd. The front and rear spar positions were fixed as in the initial geometry. The wing structural model was substituted with shell elements.

The design variables were related to airfoil, twist, and wing dihedral. The airfoil was defined at three spanwise cross-sections using the modified PARSEC model[6] with nine design variables ($x_{up}, z_{up}, z_{xx_{up}}, x_{lo}, z_{lo}, z_{xx_{lo}}, \alpha_{TE}, \beta_{TE}$, and $r_{LE_{lo}}/r_{LE_{up}}$) for each cross-section as shown in Fig. 1. The twists were defined at six spanwise locations, and wing dihedral was defined at kink and tip locations. In the present study, the twist center was set on the trailing edge. The entire wing shape was thus defined using 35 design variables. The detail of design variables is summarized in Table 1. In the present study, the surface geometry of each individual was generated using the unstructured dynamic mesh method[7] to modify the initial geometry.

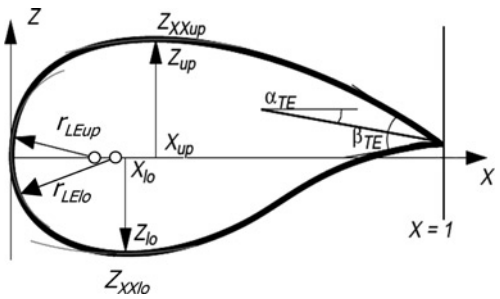

Fig. 1 Illustration of the modified PARSEC airfoil shape defined by nine design variables.

Table 1 Detail of design variables.

Serial number		Correspondent design variable
1 to 9	PARSEC airfoil	35.0% semispan location ($x_{up}, z_{up}, z_{xx_{up}}, x_{lo}, z_{lo}, z_{xx_{lo}}, \alpha_{TE}, \beta_{TE}, r_{LE_{lo}}/r_{LE_{up}}$)
10 to 18	PARSEC airfoil	55.5% semispan location
19 to 27	PARSEC airfoil	77.5% semispan location
28 to 33	Twist angle	19.3%, 27.2%, 35.0%, 55.5%, 77.5%, 96.0%
34, 35	Dihedral	35.0%, 96.0%

C. Optimizer

Adaptive range multi-objective genetic algorithm (ARMOGA)[8] was used as the optimizer. It is an efficient multi-objective evolutionary algorithm (MOEA) designed for the present multidisciplinary design optimization (MDO) problems that involves evaluations with large computational time for aerodynamic and aeroelastic evaluations. ARMOGA can find non-dominated solutions efficiently because of the focused search in design space, while maintaining diversity.[9]

D. Optimization Results

The population size was set on eight, and roughly 70 Euler and 90 Reynolds-averaged Navier-Stokes (RANS) computations were performed in one generation for computational fluid dynamics (CFD) evaluation. it took roughly one and nine hours of CPU time on NEC SX-5 and SX-7 vector machines per processing element (PE) for one Euler and RANS computation, respectively. The population was re-initialized every five generations for range adaptation. First, evolutionary computation was performed for 17 generations. Then, it was restarted using eight non-dominated solutions extracted from all solution of 17 generations, and two more generations were evolved. A total evolutionary computation of 19 generations was carried out, resulting in 130 individuals included in nine non-dominated solutions. Although the evolution had not converged, the results were satisfactory because several non-dominated solutions had achieved significant improvement over the initial design. Furthermore, the number of solutions was sufficient to perform the sensitivity analysis of the design space around the initial design. This will provide useful information for designers.

III. Data Mining Techniques

When an optimization problem has only two objective functions, tradeoff can be visualized easily. However, when there are more than two objectives, technique to visualize evaluation results and non-dominated solutions is needed. In the present study, SOM and ANOVA were employed as data mining technique. Data mining and knowledge discovery which involve data that cannot be treated using statistical analysis are new field in extracting the knowledge from database. It has the sense to transform analytical results into the concrete proposal.

A. Self-Organizing Map

SOM is a technique not only for visualization but also for intelligent compression of information. That is, SOM can be applied for data mining to acquire knowledge in the design space. In this study, Viscovery® SOMine 4.0 plus[‡] produced by Eudaptics GmbH was employed.

1. Neural Network and SOMs

SOM is a two-dimensional array of neurons:

$$\boldsymbol{M} = \left\{\boldsymbol{m}_1 \cdots \boldsymbol{m}_{p\times q}\right\} \tag{1}$$

One neuron is a vector called the codebook vector:

$$\boldsymbol{m} = \left[m_{i_1} \cdots m_{i_n}\right] \tag{2}$$

This has the same dimension as the input vectors. The neurons are connected to adjacent neurons by a neighborhood relation. This dictates the topology, or the structure, of the map. Usually, the neurons are connected to each other *via* rectangular or hexagonal topology as shown in Fig. 2. One can also define a distance between the map units according to their topology relations. Immediate neighbors (the neurons that are adjacent) belong to the neighborhood N_c of the neuron $\boldsymbol{m}_c$. The neighborhood function should be a decreasing function of time:

$$N_c = N_c(t) \tag{3}$$

The training consists of drawing sample vectors from the input data set and "teaching"the SOM. It also consists of choosing a winner unit based on a similarity measure and updating the values of codebook vectors in the neighborhood

[‡] "Eudaptics"available online at http://www.eudaptics.com [cited 16 June 2004].

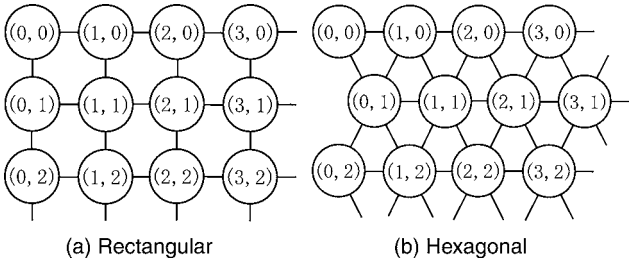

Fig. 2 Different topologies used in SOMs.

of the winner unit. This process is repeated a number of times. In one training step, one sample vector is drawn randomly from the input data set. This vector is fed to all units in the network and a similarity measure is calculated between the input data sample and all the codebook vectors. The codebook vector with greatest similarity with the input sample is chosen to be the best-matching unit. The similarity is usually defined by means of a distance measure. For example, in the case of Euclidean distance, the best-matching unit is the closest neuron to the sample in the input space.

The best-matching unit, usually noted as $\boldsymbol{m}_c$, is the codebook vector that matches a given input vector $\boldsymbol{x}$ best. It is defined formally as the neuron for which

$$\|\boldsymbol{x} - \boldsymbol{m}_c\| = \min_i [\|\boldsymbol{x} - \boldsymbol{m}_i\|] \tag{4}$$

After finding the best-matching unit, units in the SOM are updated. During the update procedure, the best-matching unit is updated to be a little closer to the sample vector in the input space. The topological neighbors of the best-matching unit are also similarly updated. This update procedure stretches the best-matching unit and its topological neighbors towards the sample vector. In the Fig. 3, the update procedure is illustrated. The codebook vectors are situated in the crossings of the solid lines. The topological relationships of the SOM are drawn with lines. The input fed to the network is marked by $\boldsymbol{x}$ in the input space. The best-matching unit, or the winner neuron is the codebook vector closest to the sample, in this example the codebook vector in the middle above $\boldsymbol{x}$. The winner neuron and its topological neighbors are updated by moving them a little towards the input sample. The neighborhood in this case consists of the eight neighboring units in the figure. The updated network is shown in the same figure with dashed lines.

2. Viscovery SOMine

Although SOMine is based on the SOM concept and algorithm, it employs an advanced variant of unsupervised neural networks, i.e. Kohonen's Batch-SOM.

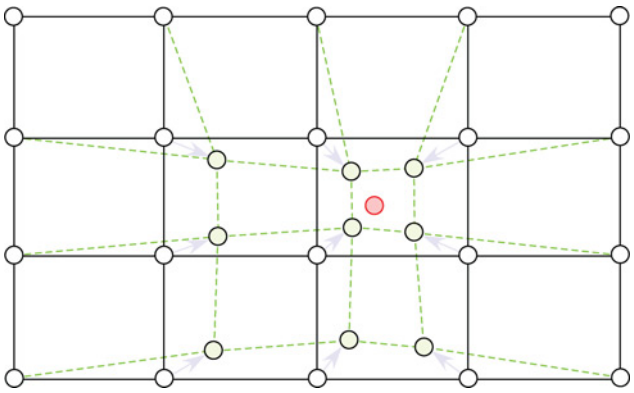

Fig. 3 Updating the best matching unit and its neighbors.

The algorithm consists of two steps that are repeated until no more significant changes occur. In the first step, the distances between all data items $\{\boldsymbol{x}_i\}$ and the model vectors $\{\boldsymbol{m}_j\}$ are computed and each data item $\boldsymbol{x}_i$ is assigned to the unit c_i that represents it best.

In the second step, each model vector is adapted to better fit the data it represents. To ensure that each unit j represents similar data items as its neighbors, the model vector $\boldsymbol{m}_j$ is adapted not only according to the assigned data items but also in regard to those assigned to the units in the neighborhood. The neighborhood relationship between two units j and k is usually defined by a Gaussian-like function

$$h_{jk} = \exp\left(-\frac{d_{jk}^2}{r_t^2}\right) \tag{5}$$

where d_{jk} denotes the distance between the units j and k on the map, and r_t denotes the neighborhood radius, which is set to decrease with each iteration t.

Assuming a Euclidean vector space, the two steps of the Batch-SOM algorithm can be formulated as

$$c_i = \arg\min \|\boldsymbol{x}_i - \boldsymbol{m}_j\| \tag{6a}$$

$$\boldsymbol{m}_j^* = \frac{\sum_i h_{jc_i}\boldsymbol{x}_i}{\sum_i h_{jc_i}} \tag{6b}$$

where $\boldsymbol{m}_j^*$ is the updated model vector.

In contrast to the standard Kohonen algorithm, which makes a learning update of the neuron weights after each record being read and matched, the Batch-SOM takes a 'batch' of data, typically all records, and performs a 'collected' update of the neuron weights after all records have been matched. This is much like 'epoch' learning in supervised neural networks. The Batch-SOM is a more robust approach, since it mediates over a large number of learning steps. Most important, no learning rate is required. The SOMine implementation combines four enhancements to the plain Batch-SOM algorithm.[10] In SOMine, the uniqueness of the map is ensured by the adoption of the Batch-SOM and the linear initialization for input data.

Much like some other SOMs,[11] SOMine creates a map in a two-dimensional hexagonal grid. Starting from numerical, multivariate data, the nodes on the grid gradually adapt to the intrinsic shape of the data distribution. Since the order on the grid reflects the neighborhood within the data, features of the data distribution can be read off from the emerging map on the grid.

In SOMine, the trained SOM is systematically converted into visual information. The tool provides an extensive built-in capability for both pre-processing and post-processing as well as for the automatic color-coding of the map and its components. SOMine is particularly useful in the determination of dependencies between variables as well as in the analysis of high-dimensional cluster distributions.

3. Cluster Analysis

Once SOM projects the input space onto a low-dimensional regular grid, the map can be utilized to visualize and explore properties of the data. When the number of SOM units is large, to facilitate quantitative analysis of the map and the data, similar units need to be clustered. Two-stage procedure—first using SOM to produce the prototypes which are then clustered in the second stage—was reported to perform well when compared to direct clustering of the data.[11]

Hierarchical agglomerative algorithm is used for clustering here. The algorithm starts with a clustering where each node by itself is a cluster. In each step of the algorithm two clusters with minimal distance are merged. The distance is the SOM-Ward distance. This measure takes into account whether two clusters are adjacent in the map. This means that the process of merging clusters is restricted to topologically adjacent clusters. The number of clusters will be different according to the hierarchical sequence of clustering. A relatively small number will be chosen for visualization, while a large number will be used for generation of codebook vectors for respective design variables.

B. Functional Analysis of Variance

Functional analysis of variance (ANOVA)[4] employs the variance of the objective functions due to the design variables on the response surface models. Thus, the response surface model should first be constructed for each objective function to calculate the variance. The response surface model employed in the present study is the kriging model.[12] The kriging model, developed in the field of spatial statistics and geo-statistics, predicts the distribution value of the unknown point by using stochastic processes. The kriging model is expressed as follows:

$$\hat{y}(\boldsymbol{x}) = \hat{\mu} + \boldsymbol{r}'\boldsymbol{R}^{-1}(\boldsymbol{y} - \boldsymbol{I}\hat{\mu}) \tag{7}$$

where $\boldsymbol{x} = \{x_1, x_2, \cdots, x_n\}$ denotes the vector of design variables, $\boldsymbol{y}$ is the column vector of sampled response data, and $\boldsymbol{I}$ is unit column vector. $\boldsymbol{R}$ is the correlation matrix whose (i, j) element is

$$R\left(\boldsymbol{x}^i, \boldsymbol{x}^j\right) = \exp\left[-\sum_{k=1}^{n} \theta_k \left|x_k^i - x_k^j\right|^2\right] \tag{8}$$

The correlation vector between $\boldsymbol{x}$ and the m sampled data is expressed as

$$\boldsymbol{r}'(\boldsymbol{x}) = \left[R\left(\boldsymbol{x}, \boldsymbol{x}^1\right), R\left(\boldsymbol{x}, \boldsymbol{x}^2\right), \cdots, R\left(\boldsymbol{x}, \boldsymbol{x}^m\right)\right] \tag{9}$$

The value $\hat{\mu}$ is estimated using the generalized least squares method as

$$\hat{\mu} = \frac{\boldsymbol{I}'\boldsymbol{R}^{-1}\boldsymbol{y}}{\boldsymbol{I}'\boldsymbol{R}^{-1}\boldsymbol{I}} \tag{10}$$

Once the response surface model is made, the effect of design variables on the objective function can be calculated by decomposing the total variance of model into the variance due to each design variable. The decomposition is performed by integrating variables out of the model $\hat{y}$. The total mean ($\hat{\mu}_{\text{total}}$) and the variance ($\hat{\sigma}^2_{\text{total}}$) of model are as follows:

$$\hat{\mu}_{\text{total}} \equiv \int \cdots \int \hat{y}\,(x_1, x_2, \ldots, x_n)\, dx_1 dx_2 \cdots dx_n \tag{11a}$$

$$\hat{\sigma}^2_{\text{total}} = \int \cdots \int \left[\hat{y}\,(x_1, x_2, \ldots, x_n) - \hat{\mu}_{\text{total}}\right]^2 dx_1 dx_2 \cdots dx_n \tag{11b}$$

The main effect of variable x_i and the two-way interaction effect of variable x_i and x_j are given as follows:

$$\hat{\mu}\,(x_i) \equiv \int \cdots \int \hat{y}\,(x_1, x_2, \ldots, x_n)\, dx_1 dx_2 \cdots dx_{i-1} dx_{i+1} \cdots dx_n - \hat{\mu}_{\text{total}} \tag{12}$$

$$\begin{aligned}\hat{\mu}_{i,j}\left(x_i, x_j\right) \equiv{}& \int \cdots \int \hat{y}\,(x_1, x_2, \ldots, x_n)\, dx_1 dx_2 \cdots dx_{i-1} dx_{i+1} \cdots dx_{j-1} dx_{j+1} \cdots dx_n \\ &- \hat{\mu}_i\,(x_i) - \hat{\mu}_j\left(x_j\right) - \hat{\mu}_{\text{total}}\end{aligned} \tag{13}$$

$\hat{\mu}(x_i)$ and $\hat{\mu}_{i,j}(x_i, x_j)$ quantify the effect of variable x_i and interaction effect of x_i and x_j on the objective function. The variance due to the design variable x_i is obtained as follows:

$$\hat{\sigma}^2_{x_i} = \int \left[\hat{\mu}_i\,(x_i)\right]^2 dx_i \tag{14}$$

The proportion of the variance P due to design variable x_i to total variance of model can be expressed by dividing Eq. (14) with Eq. (11b).

$$P = \frac{\hat{\sigma}^2_{x_i}}{\hat{\sigma}^2_{\text{total}}} = \frac{\int \left[\hat{\mu}_i\,(x_i)\right]^2 dx_i}{\int \cdots \int \left[\hat{y}\,(x_1, x_2, \ldots, x_n) - \hat{\mu}_{\text{total}}\right]^2 dx_1 dx_2 \cdots dx_n} \tag{15}$$

This value indicates the effect of design variable x_i on the objective function.[13]

IV. Data Mining Results

A. Knowledge Extracted by SOM

1. *Tradeoff Analysis of the Design Space*

All solutions have been projected onto the two-dimensional map of SOM. Figure 4 shows the generated SOM with 11 clusters taking the three objective functions into consideration. Fig. 5 shows the SOMs colored by the three objective functions. These color figures show that the SOM indicated in Fig. 4 can be grouped as follows: The upper left corner corresponds to the individuals with high block fuel and maximum takeoff weight. The center left area corresponds to the individuals with high maximum takeoff weight and C_D divergence. The lower left corner corresponds to the individuals with low block fuel and high C_D divergence. That is, Figs. 5(a) and 5(b) have a color pattern of decreasing the objective function values from upper left to lower right. On the other hand, Fig. 5(c) has a color pattern of decreasing from lower left to upper right. Therefore, there is no tradeoff between the block fuel and the maximum takeoff weight. There are tradeoffs between the C_D divergence and the other objective functions.

Figure 5 shows that the cluster on the lower right corner has the individuals with low values of all objective functions. That is, there is a sweet spot in this design space. On the other hand, extreme solutions, which mean the champions (or best solutions) for each objective function, exist on the different location in Fig. 5. Therefore, although there is a sweet spot, it is impossible to simultaneously minimize all objective functions in this design space.

2. *Effects of Aerodynamic Performance on Objective Functions*

Figure 6 shows the SOMs colored by the transonic aerodynamic performance. Figures 6(a) and 6(b) show the SOMs colored by C_L and C_D, respectively. Similar color pattern between these indicates that the increase of L/D is difficult. Low C_D values are located in the lower right corner in Fig. 6(b). As this area clusters the designs with low values of all objective functions, this suggests that transonic C_D is also reduced when all objective functions are optimized simultaneously. That is, decrease of C_D is important to generate a solution in the sweet spot. Furthermore, as the clusters of low values of the maximum takeoff weight shown in Fig. 5(b) appear on the right hand side of the map, decrease of C_D gives effect on the maximum takeoff weight. As the area with high C_D shown in Fig. 6(b) generally coincide with the area with high objective function values, C_D is an important performance index.

Figure 6(c) shows the SOM colored by L/D. This figure shows that low values of L/D are located in the upper left corner. As the high values of the block fuel shown in Fig. 5(a) are present at the similar location, low L/D increases the block fuel. Furthermore, high L/D values are located in the lower area shown in Fig. 6(c). As the low values of the block fuel shown in Fig. 5(a) are present at the similar area, high L/D is effective to decrease the block fuel. In this study, since the block fuel is computed by using L/D at subsonic, transonic, and off-design conditions, and also structural weight, the increases of L/D at all flight conditions are important to reduce the block fuel.

Figure 6(d) shows the SOM colored by C_{Mp}. When C_{Mp} increases, L/D is reduced. C_L and C_D increase with decreasing C_{Mp}. The decrease of C_{Mp} gives worse effect on the objective functions.

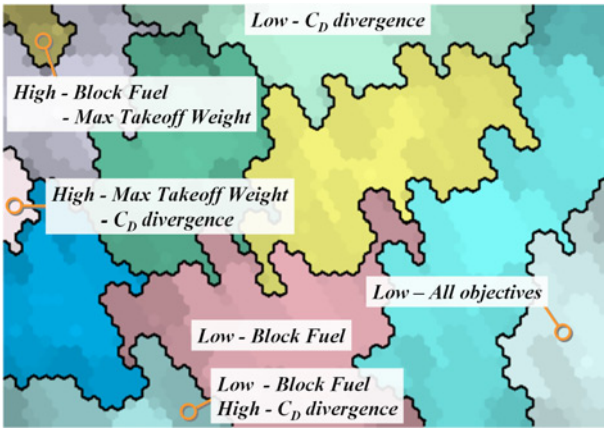

Fig. 4 SOM of all solutions in the three-dimensional objective function space.

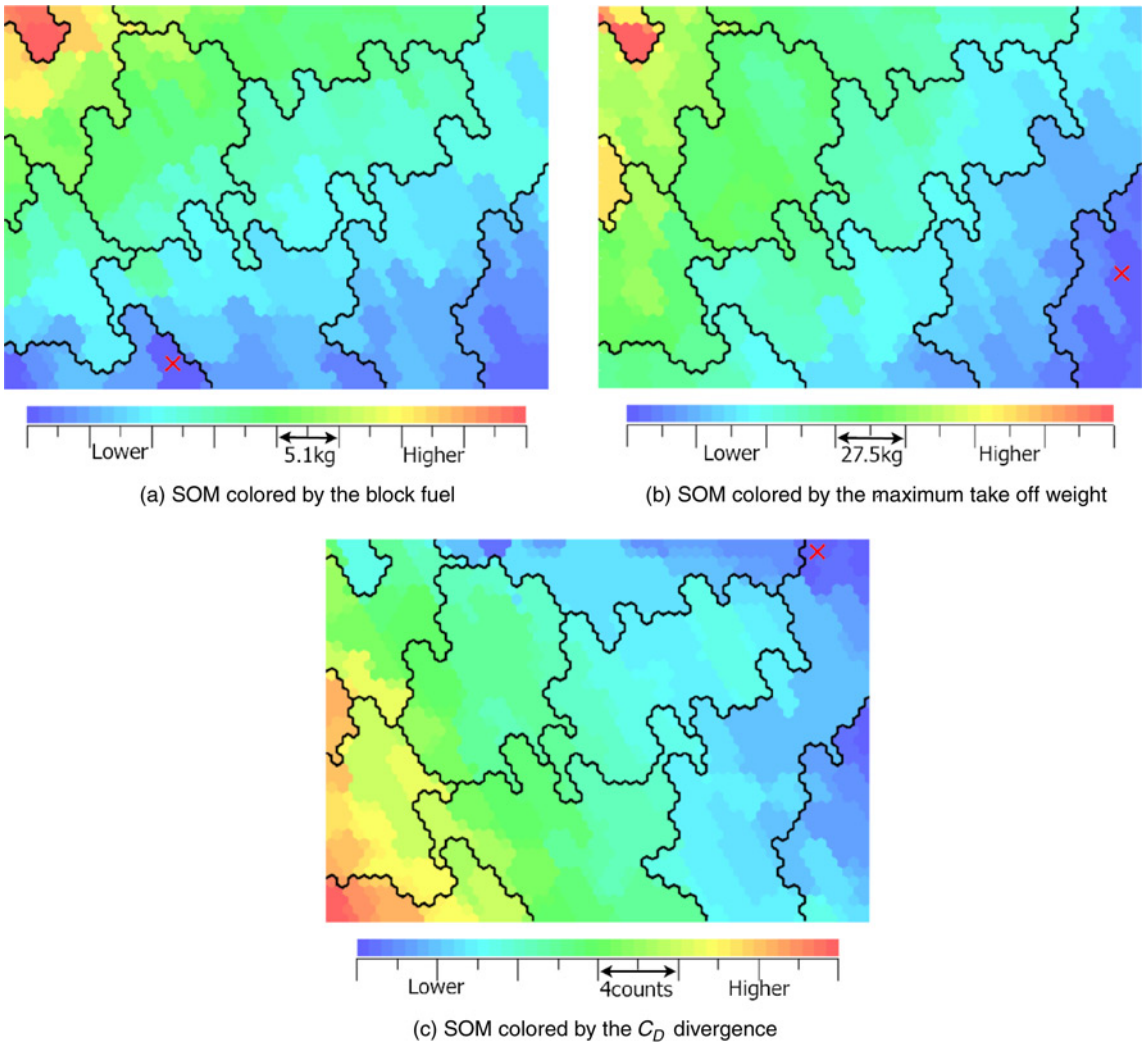

Fig. 5 SOM colored according to the objective functions. The symbol × denotes the respective extreme non-dominated solutions.

Figure 7 shows the SOM colored by subsonic C_L and C_D. As the resulting SOMs appear similar to transonic C_L and C_D shown in Fig. 6(a) and 6(b), subsonic aerodynamic performance gives similar effect on the objective functions compared with the transonic aerodynamic performance. That is, the effects of subsonic aerodynamic performance on the objective functions are predicted from the effects of transonic aerodynamic performance in this study.

3. Additional Characteristics

The SOMs colored by three characteristic values are shown in Fig. 8. Figure 8(a) shows the SOM colored by the value of $V_{\text{required fuel}} - V_{\text{fuel capacity}}$. $V_{\text{required fuel}}$ denotes the fuel volume required to fly at a given range, and $V_{\text{fuel capacity}}$ denotes the fuel capacity volume which can be practically carried in the wing. When this value is greater than zero, the aircraft cannot fly for the given range. As the area with positive values corresponds to that with high maximum takeoff weight, the aerodynamic characteristics and design variables which give effects on maximum takeoff weight dominate this constraint.

Figure 8(b) shows the SOM colored by the rank in the optimizer. As the upper left region clusters the solutions with the bad rank, larger block fuel and maximum takeoff weight dominate these solutions. However, the lower left

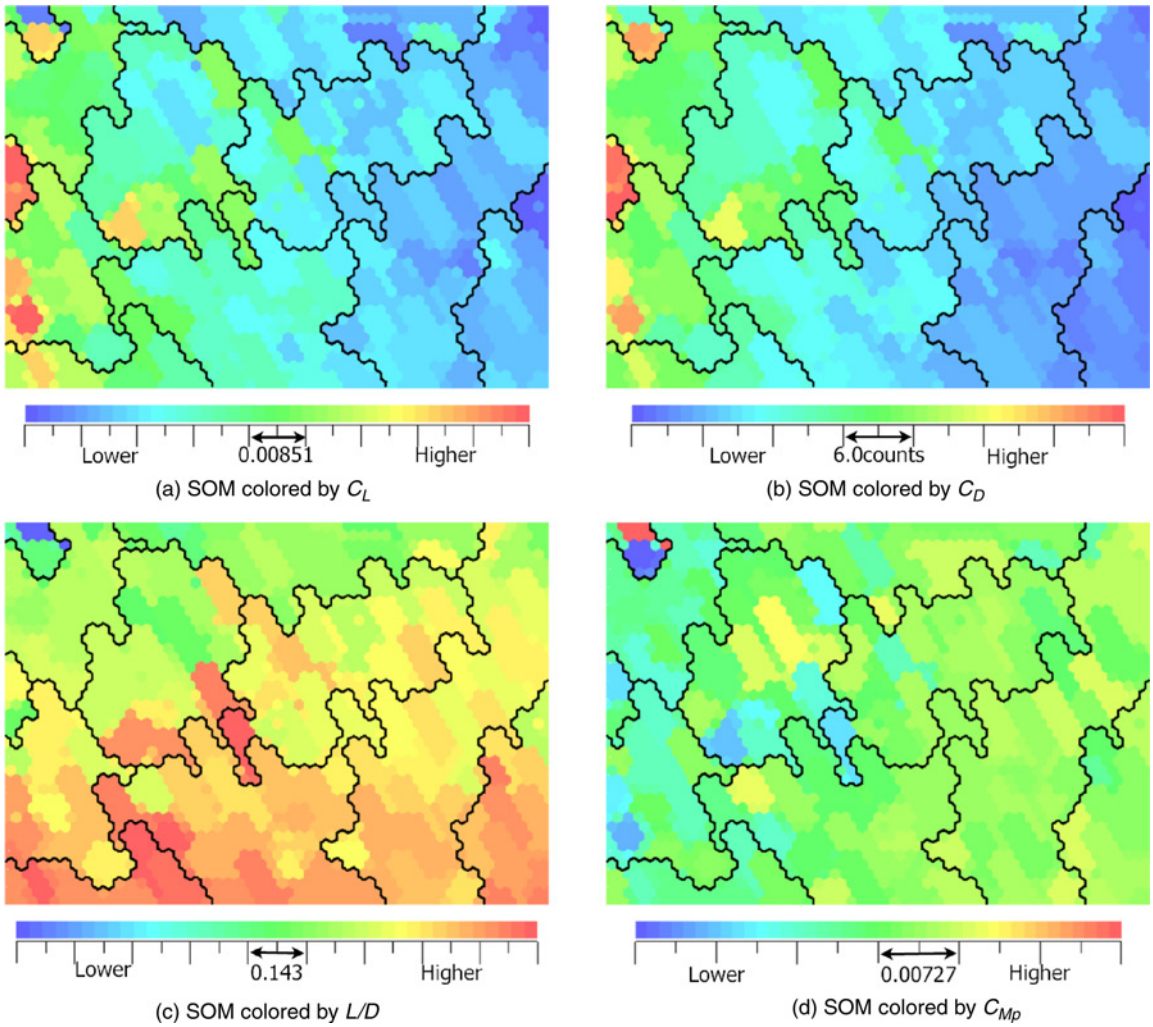

Fig. 6 SOM colored by aerodynamic performance under transonic cruising flight condition.

area with high C_D divergence does not have bad rank. This fact indicates that improvement in C_D divergence is not dominated by specific values (for example, aerodynamic/structural characteristics and design variables). Therefore, further improvement cannot be easily achieved by the present problem.

Figure 8(c) shows the SOM colored by the angle between inboard and outboard wings on the upper surface. Greater angle than 180 deg represents gull-wing, and lower angle than 180 deg describes inverted gull-wing. The locations of high values of this angle as shown in Fig. 8(c) correspond to those of high transonic C_D shown in Fig. 6(b). However, there is no color pattern regarding the values of lower than 180 deg in Fig. 8(c). Therefore, it indicates that the inverted gull-wing does not affect the aerodynamic characteristics. As it is known that no-straight wing gives effect to increase structural weight, non-gull-wing (straight wing) can reduce structural weight while aerodynamic performances are kept.

4. Effects of Design Variables

Figures. 9 and 10 show the SOMs colored by the selected design variables with regard to the PARSEC airfoil parameters at 35.0% and 55.5% spanwise locations, respectively. In addition, Fig. 11 shows the SOMs colored by the twist angles. These figures show that there is no design variable which shows large effects on the block fuel as the primary objective function. The large twist angles at the 35.0% spanwise location gives worse effect on the

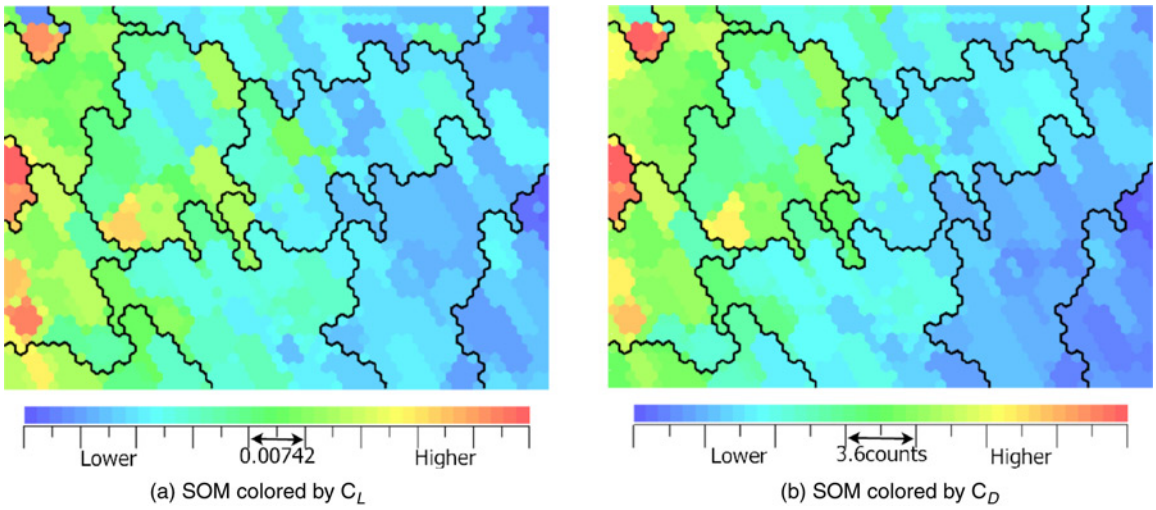

Fig. 7 SOM colored by aerodynamic performance under subsonic flight condition.

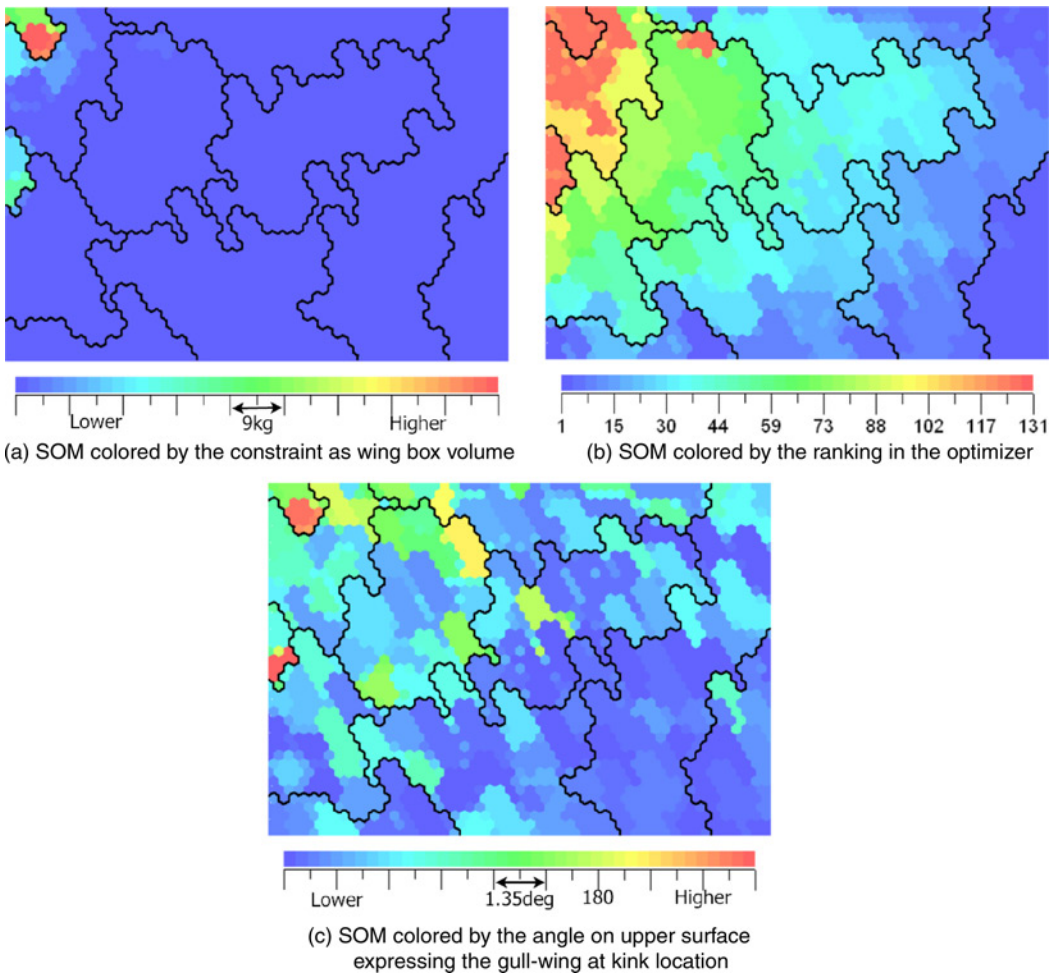

Fig. 8 SOM colored by the characteristic values.

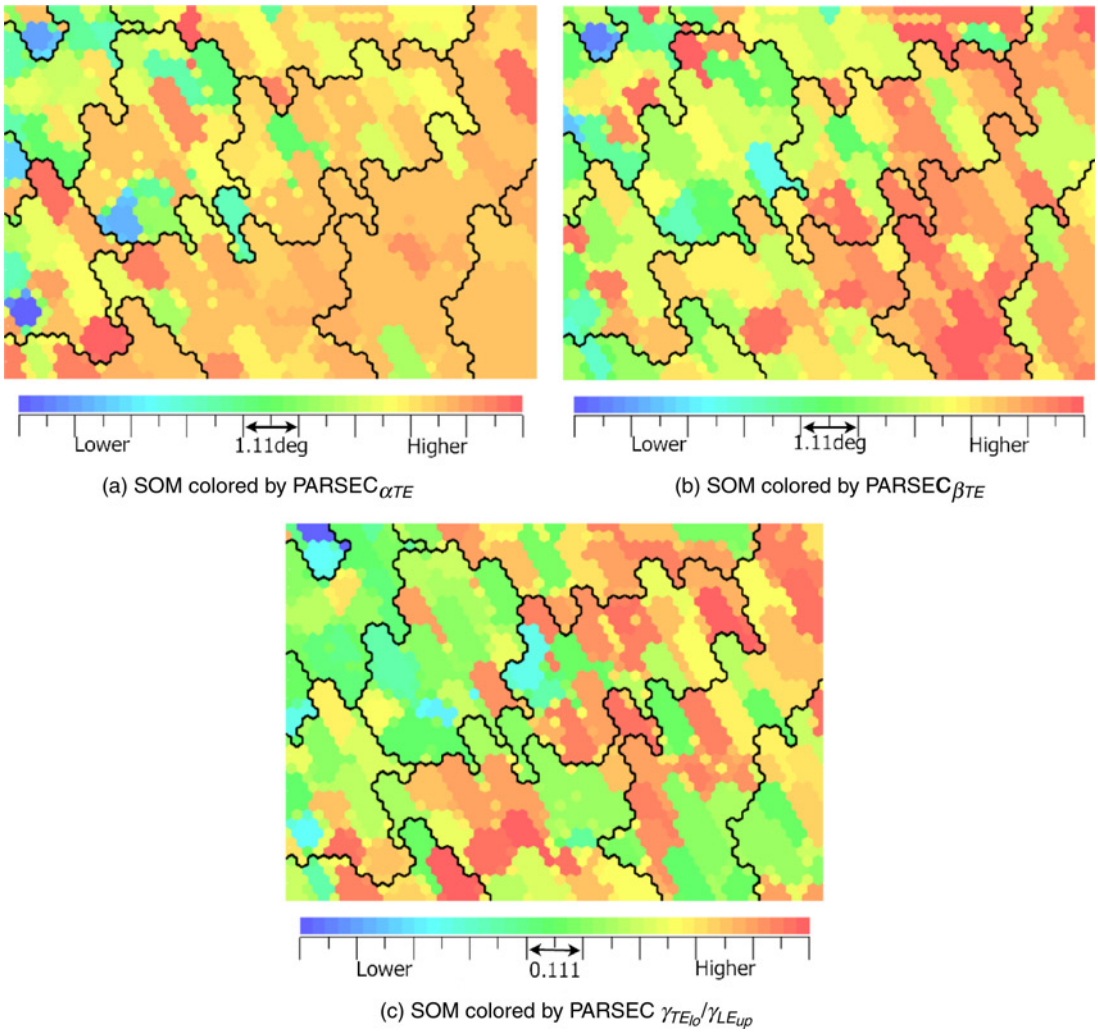

Fig. 9 SOM colored by characteristic design variables regarding the PARSEC airfoil at 35.0% spanwise location. The minimum and maximum values of color bar are set using the minimum and maximum values of each design variable in optimizer, respectively.

maximum takeoff weight shown in Fig. 11(a). The large twist angles at the 55.5% spanwise location increase C_D divergence. However, there is no design variable regarding the PARSEC airfoil to give effects on any objective functions. PARSEC design variables directly give effects on aerodynamic performances. But, the present objective functions are not defined by pure aerodynamic characteristics. Therefore, effects of the PARSEC design variables on the objective functions were not directly appeared. As there were no specific design variable and no aerodynamic characteristic which gave effects on the solutions in the sweet spot, it is difficult to artificially generate the solution in the sweet spot using the control of the present design variables. Although knowledge discovery regarding the correlation between objective function and design variable is important to solve a multi-objective optimization problem, it depends on the definition of design variable. When the multidisciplinary objective function is considered, the definition using peculiar design variables for transonic aerodynamic performance like PARSEC does not explicitly give design knowledge.

Next, the effective design variables to aerodynamic performance are investigated. The obtained knowledge regarding the effects of respective design variables are summarized in Tables 2 to 4. These indicate that the design

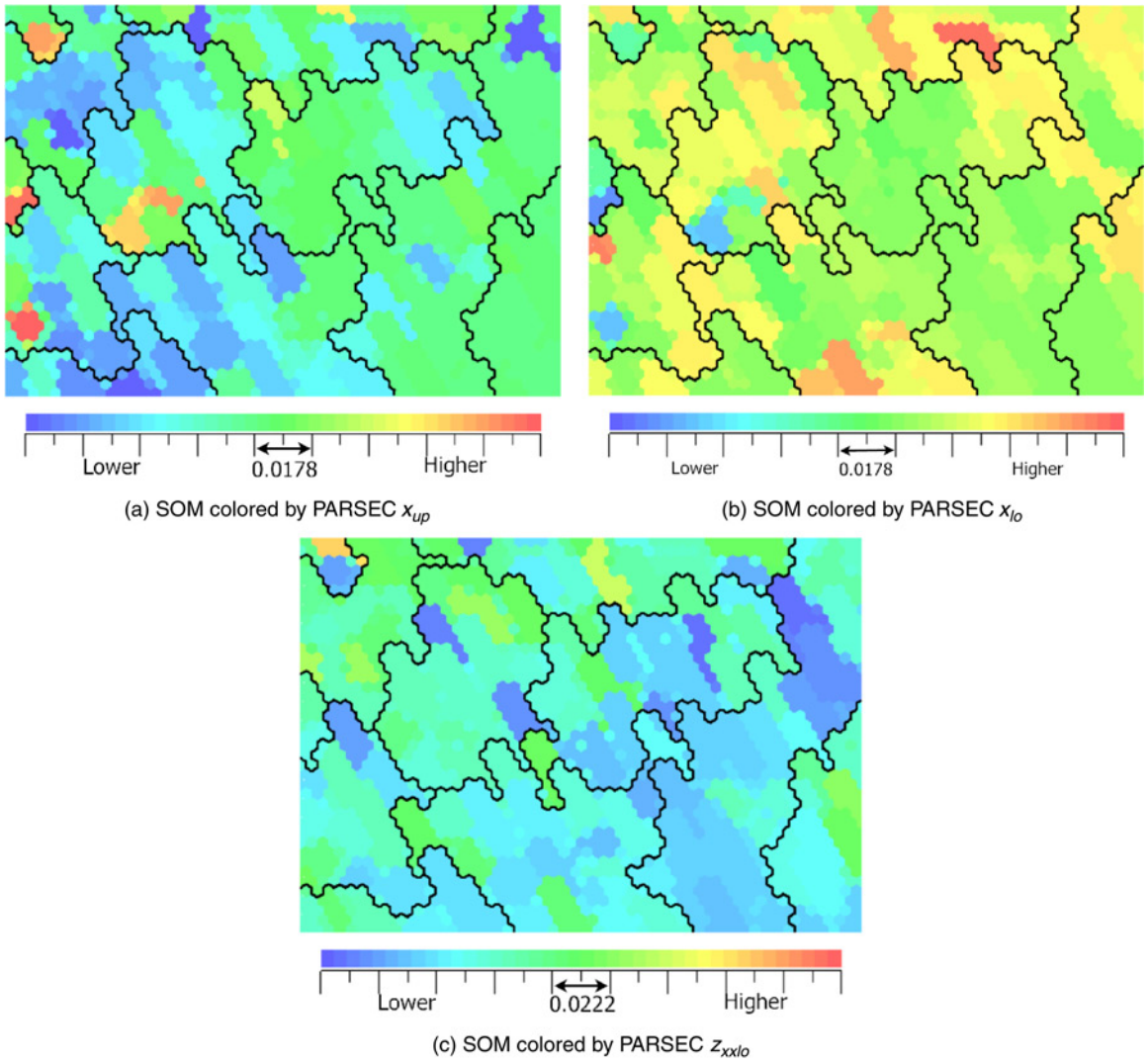

Fig. 10 SOM colored by the characteristic design variables regarding the PARSEC airfoil at 55.5% spanwise location. The minimum and maximum values of color bar are set using the minimum and maximum values of each design variable in optimizer, respectively.

variables of the PARSEC airfoil give effects on aerodynamic performance directly as it expected. It is notable that the effects of design variables to C_D can be predicted as similar effects to C_L indicated in Table 2 because Figs. 6(a) and (b) are similar color pattern. Furthermore, the effects of design variable on subsonic aerodynamic performance can be predicted because of the similar SOM color pattern between transonic and subsonic conditions as shown in Figs. 6 and 7. Figure 9(c) shows that the low value of $r_{LE_{lo}}/r_{LE_{up}}$ of PARSEC airfoil at 35.0% spanwise location gives effect on the decrease of L/D and the increase of C_{Mp} at subsonic and transonic conditions.

The twist angle near 55.5% spanwise location is not markedly changed as shown in Fig. 11(b). This indicates that the twist angle at 55.5% spanwise location does not have to shift to improve the objective functions. The twist angle near 35.0% spanwise location is changed to downward. On the other hand, the twist angle near 96.0% spanwise location is shifted to upward. The angle of attack of the inboard wing, whose size is larger than that of the outboard wing, is twisted down so that the wave drag near the kink is reduced. However, it is predicted by the knowledge

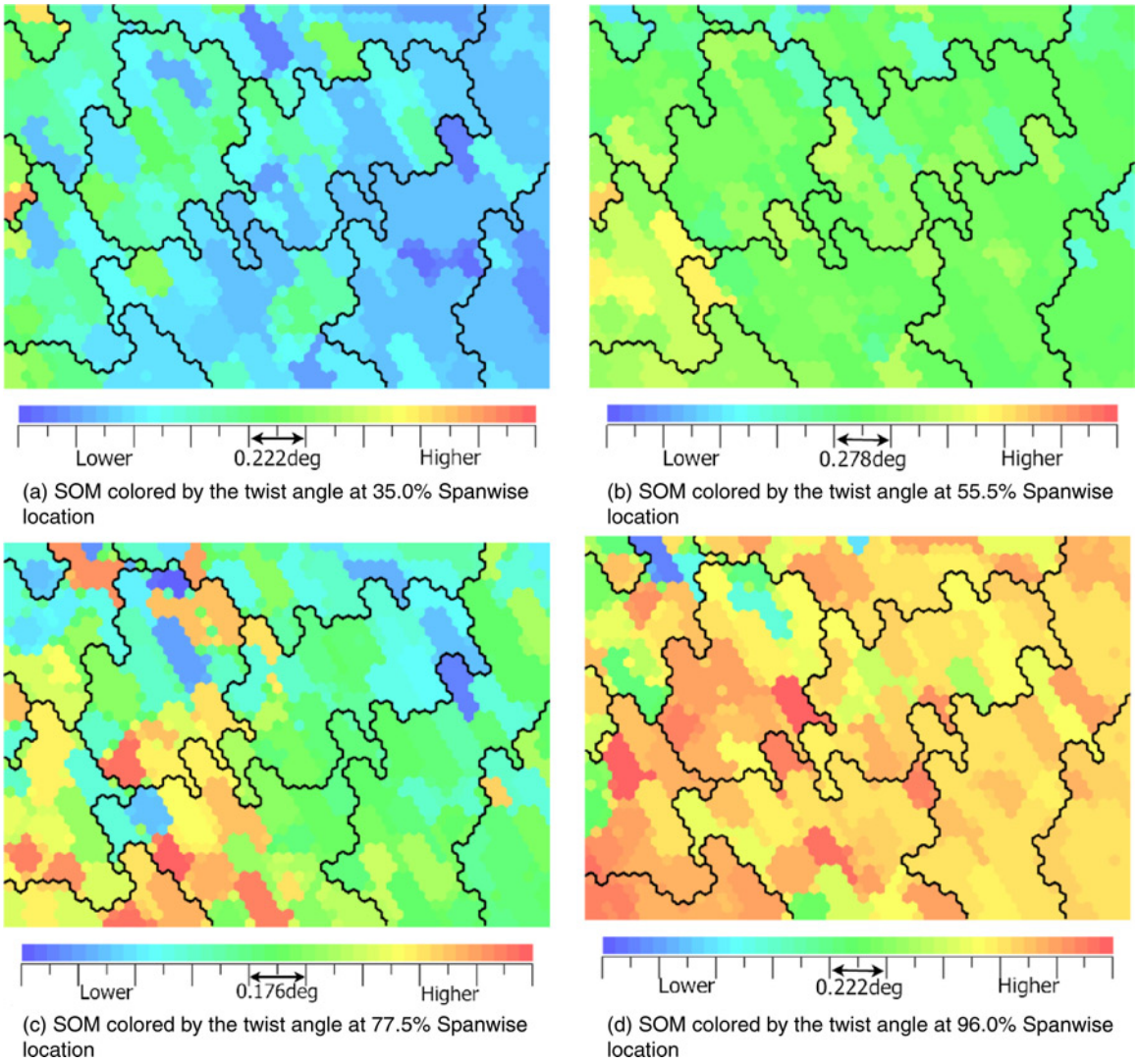

Fig. 11 SOM colored by the characteristic design variables involving wing twist. The minimum and maximum values of color bar are set using the minimum and maximum values of each design variable in optimizer, respectively.

Table 2 Effects of design variables to C_L under transonic cruising flight condition.

Design variable		C_L
PARSEC α_{TE} @ 35.0%	decrease	increase
PARSEC x_{up} @ 55.5%	increase	increase
PARSEC x_{lo} @ 55.5%	decrease	increase
Twist @ 35.0%	increase	increase
Twist @ 55.5%	increase	increase

Table 3 Effects of design variables to *L/D* under transonic cruising flight condition.

Design variable		L/D
PARSEC $r_{LE_{lo}}/r_{LE_{up}}$ @ 35.0%	decrease	decrease
PARSEC $z_{xx_{lo}}$ @ 55.5%	increase	decrease

Table 4 Effects of design variables to C_{Mp} under transonic cruising flight condition.

Design variable		C_{Mp}
PARSEC α_{TE} @ 35.0%	decrease	decrease
PARSEC β_{TE} @ 35.0%	decrease	decrease
PARSEC $r_{LE_{lo}}/r_{LE_{up}}$ @ 35.0%	decrease	increase
PARSEC x_{up} @ 55.5%	increase	decrease
PARSEC x_{lo} @ 55.5%	decrease	decrease
PARSEC $z_{xx_{lo}}$ @ 55.5%	increase	increase

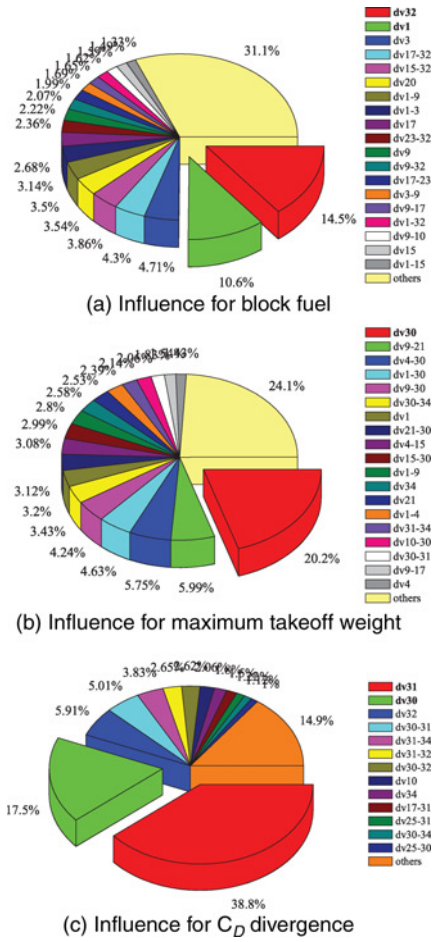

Fig. 12 Proportion of design-variable influence for the objective functions using ANOVA.

from SOM that the lift near the inboard wing is also reduced. Therefore, the angle of attack of the outboard wing is twisted up to compensate the lift. It is notable that the twist-up of the outboard wing does not give large effect on the transonic drag shown in Figs. 11(c) and (d).

The effects of the design variables on the aerodynamic performance indicate that the increases of L/D and $dC_D/d\alpha$ at any Mach numbers are essential to improve the block fuel as the primary objective function. However, there is no design variable to directly improve them.

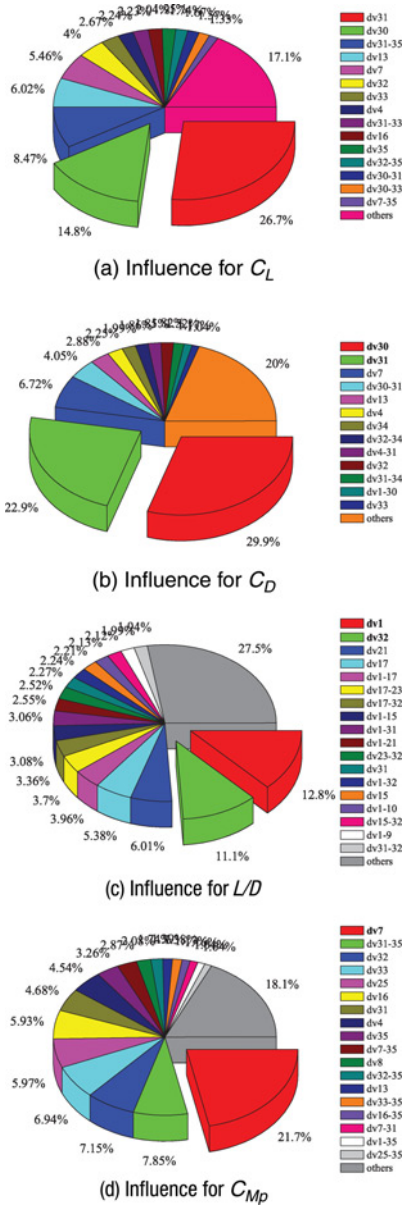

Fig. 13 Proportion of design-variable influence for aerodynamic performance at the transonic cruising condition using ANOVA.

Table 5 Comparison of the most influential design variable for the objective functions between ANOVA and SOM.

	ANOVA	SOM
block fuel	Twist @ 77.5%	—
max takeoff weight	Twist @ 35.0%	Twist @ 35.0%
C_D divergence	Twist @ 55.5%	Twist @ 55.5%

B. Knowledge Extracted by ANOVA

Figures 12 and 13 show the proportion of the effects of design variables for the objective functions and aerodynamic performance obtained by ANOVA. The effects of the design variables for each objective function obtained by ANOVA and SOM are summarized in Table 5. This table shows that ANOVA and SOM predict similar influence for the maximum takeoff weight and the C_D divergence. As these two objective functions have correlation with aerodynamic performance, the specific effects of the design variables appear for them. However, the block fuel does not have a correspondent result between ANOVA and SOM. As the block fuel is computed from the wing structural weight and L/D at subsonic, transonic, and off-design conditions, it is sensitive to various elements. When the effect of design variable is investigated, the definition manner of design variable is important.

The disadvantages of ANOVA and SOM would be investigated. Although ANOVA can explicitly address the effective design variables, it is indistinct how an addressed design variable gives effect on an objective function. Whereas, the disadvantages of SOM are 1) qualitatively and subjective. 2) possible to overlook design knowledge because of a large number of objective functions and design variables, and 3) the interaction between the design variables cannot be investigated directly. Therefore, when data mining is performed by SOM after sensitive design variables are addressed by ANOVA, they can compensate with the respective disadvantages.

C. Evaluation of an Improved Geometry

The design knowledge obtained by data mining shows that straight wing should be designed. Therefore, the optimized wing shape (called as '*optimized*' shown in Fig.14), which achieved the higher improvement in the block fuel, is modified to the non-gull wing shape (called as '*optimized_mod*').

The evaluated results are shown in Figs. 14 to 16. These figures show that *optimized_mod* largely improves both of the block fuel and the maximum takeoff weight. Moreover, transonic C_D of *optimized_mod* was found to be reduced by 10.6 counts over the initial geometry from C_L-C_D polar curves. The block fuel of $optimized\_mod$ was reduced by 3.6 percent due to the reduction of drag.

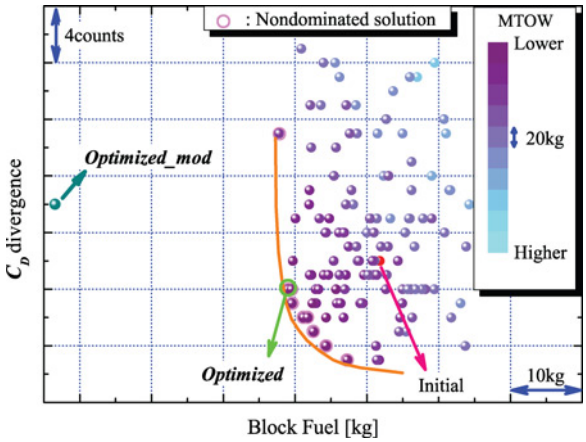

Fig. 14 Comparison of *optimized_mod* and all solutions on two-dimensional plane between block fuel and C_D divergence.

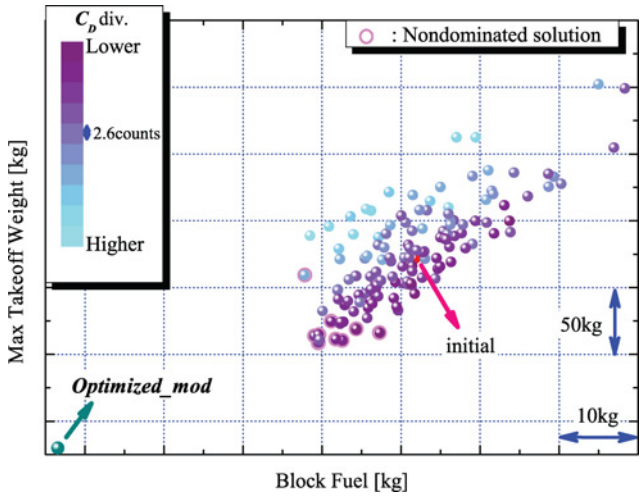

Fig. 15 Comparison of *optimized_mod* and all solutions on two-dimensional plane between block fuel and maximum takeoff weight.

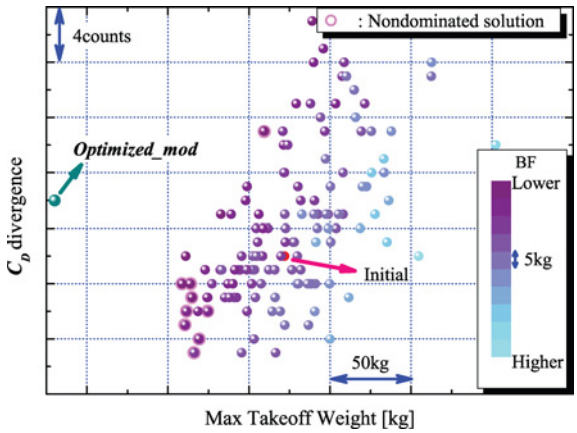

Fig. 16 Comparison of *optimized_mod* and all solutions on two-dimensional plane between maximum takeoff weight and C_D divergence.

In this MDO system, surface spline function of the geometry deviation was used for the modification of the wing shape (surface mesh) by the unstructured dynamic mesh method, and then the volume mesh was re-generated. However, this process made the surface mesh distorted around the leading edge and highly limited the design space. This mesh generation process might be the primary reason for the difficulty in finding the non-gull geometry with better block fuel performance. The secondary reason is that only the small number of the generations was performed. However, data mining salvages this information. It is demonstrated that the knowledge discovery by data mining is an important aspect in the practical optimization.

V. Conclusion

Data mining has been performed using SOM and ANOVA for a large-scale and real-world MDO results to provide the design knowledge. As a result, SOM reveals the tradeoffs among objective functions. Moreover, SOM roughly addresses the effective design variables and also it reveals how an addressed design variable gives effect on objective functions and various characteristics. The high value of 35.0% twist angle increases the maximum takeoff weight. The high value of 55.5% twist angle increases C_D divergence. No design variable has direct effects on the block

fuel. There is a sweet spot in the present design space. Whereas, ANOVA explicitly addresses the effective design variables. The result of ANOVA for the block fuel does not correspond to that of SOM. As the block fuel is computed from various characteristics, the reliability of results by ANOVA decreases. The combination of SOM and ANOVA compensate with the respective disadvantages.

Although the present MDO results showed the inverted gull-wings as non-dominated solutions, one of the key features found by data mining was the straight wing geometry. When this knowledge was applied to one optimum solution, the resulting solution was found to have better performance compared with the original geometry designed in the conventional manner. Consequently, data mining can discover better design due to the salvage of information from design space even when optimization itself does not converge.

References

[1]Holden, C. M. E. and Keane, A. J., "Visualization Methodologies in Aircraft Design," AIAA Paper 2004-4449, 2004.

[2]Obayashi, S. and Sasaki, D., "Visualization and Data Mining of Pareto Solutions Using Self-Organizing Map," *The 2nd International Conference on Evolutionary Multi-Criterion Optimization, LNCS 2632*, Springer-Verlag Heidelberg, Faro, Portugal, 2003, pp. 796–809.
doi: 10.1007/3-540-36970-8_56

[3]Kohonen, T., *Self-Organizing Maps*, Springer, Berlin, Heidelberg, 1995.

[4]Jones, D. R., Schonlau, M., and Welch, W. J., "Efficient Global Optimization of Expensive Black-Box Functions," *Journal of Global Optimization*, Vol. 13, No. 4, 1998, pp. 455–492.

[5]Chiba, K., Oyama, A., Obayashi, S., Nakahashi, K., and Morino, H., "Multidisciplinary Design Optimization and Data Mining of Transonic Regional-Jet Wing," *Journal of Aircraft*, Vol. 44, No. 4, 2007, pp. 1100–1112.

[6]Oyama, A., Obayashi, S., Nakahashi, K., and Hirose, N., "Aerodynamic Wing Optimization via Evolutionary Algorithms Based on Structured Coding," *Computational Fluid Dynamics Journal*, Vol. 8, No. 4, 2000, pp. 570–577.

[7]Yamazaki, W., Matsushima, K., and Nakahashi, K., "Aerodynamic Optimization of NEXST-1 SST Model at Near-Sonic Regime," AIAA Paper 2004-0034, 2004.

[8]Sasaki, D. and Obayashi, S., "Efficient Search for Trade-Offs by Adaptive Range Multi-Objective Genetic Algorithms," *Journal of Aerospace Computing, Information, and Communication*, Vol. 2, No. 1, 2005, pp. 44–64.

[9]Sasaki, D., Obayashi, S., and Nakahashi, K., "Navier-Stokes Optimization of Supersonic Wings with Four Objectives Using Evolutionary Algorithm," *Journal of Aircraft*, Vol. 39, No. 4, 2002, pp. 621–629.

[10]Deboeck, G. and Kohonen, T., *Visual Explorations in Finance with Self-Organizing Maps*, Springer Finance, London, 1998.

[11]Vesanto, J. and Alhoniemi, E., "Clustering of the Self-Organizing Map," *IEEE Transactions on Neural Networks*, Vol. 11, No. 3, 2000, pp. 586–600.

[12]Keane, A. J., "Wing Optimization Using Design of Experiment, Response Surface, and Data Fusion Methods," *Journal of Aircraft*, Vol. 40, No. 4, 2003, pp. 741–750.

[13]Jeong, S., Murayama, M., and Yamamoto, K., "Efficient Optimization Design Method Using Kriging Model," *Journal of Aircraft*, Vol. 42, No. 2, 2005, pp. 413–420.

J. A. Mulder
Associate Editor